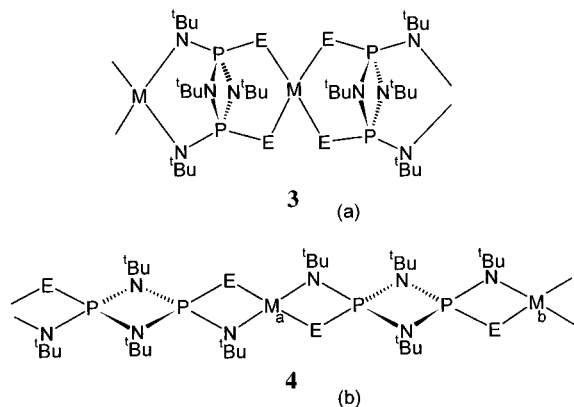


**Scheme 1.** Metal-Containing Polymers Containing the Dianions **2a** and **2b**:(a) *N,N'* and *E,E'* Chelation and (b) Bis(*N,E*) Chelation

none); acetonitrile ( $P_2O_5$ ). The reagents *cis*-PtCl<sub>2</sub>(PEt<sub>3</sub>)<sub>2</sub> (99%, Strem), PdCl<sub>2</sub>(PhCN)<sub>2</sub> (99%, Strem), *trans*-PdCl<sub>2</sub>(PPh<sub>3</sub>)<sub>2</sub> (99%, Strem), and CuCl (99.99+%, Aldrich) were used as received. The compounds {(THF)<sub>2</sub>Li[(<sup>t</sup>BuN)(S)P( $\mu$ -N'<sup>t</sup>Bu)<sub>2</sub>P(S)(NH<sup>t</sup>Bu)]} (**10**)<sup>6b</sup> and NiCl<sub>2</sub>(PEt<sub>3</sub>)<sub>2</sub><sup>8</sup> were prepared by literature procedures. The handling of air- and moisture-sensitive reagents was performed under an atmosphere of argon gas using Schlenk techniques or a glovebox.

**Instrumentation.** <sup>1</sup>H NMR spectra were collected on a Bruker AM-200 spectrometer, and chemical shifts are reported relative to Me<sub>4</sub>Si in CDCl<sub>3</sub>. <sup>31</sup>P NMR were recorded on a Varian XL-200 MHz spectrometer; chemical shifts are reported relative to 85% H<sub>3</sub>PO<sub>4</sub> in D<sub>2</sub>O. <sup>195</sup>Pt NMR was recorded on a Bruker AMX-300 spectrometer; chemical shifts are reported relative to 0.2 M H<sub>2</sub>PtCl<sub>6</sub> in D<sub>2</sub>O. IR spectra were recorded as Nujol mulls between KBr plates on a Mattson 4030 FTIR spectrometer in the range 4000–350 cm<sup>-1</sup>. Electron-impact mass spectra were obtained by using a VG7070F spectrometer operating at 70 eV. UV–vis spectra were collected on a Unicam Helios UV-visible spectrometer in the range 190–720 nm. Elemental analyses were determined by the Analytical Services Laboratory, Department of Chemistry, University of Calgary.

**Preparation of {(PPh<sub>3</sub>)<sub>2</sub>Cu[(<sup>t</sup>BuN)(S)P( $\mu$ -N'<sup>t</sup>Bu)<sub>2</sub>P(S)(NH<sup>t</sup>Bu)]} (**5**).** A solution of CuCl (0.09 g, 0.44 mmol) in MeCN (30 mL) was added to a stirred solution of {(THF)<sub>2</sub>Li[(<sup>t</sup>BuN)(S)P( $\mu$ -N'<sup>t</sup>Bu)<sub>2</sub>P(S)(NH<sup>t</sup>Bu)]} (0.50 g, 0.89 mmol) and PPh<sub>3</sub> (0.23 g, 0.44 mmol) dissolved in MeCN (25 mL) at 23 °C. After 18 h, removal of the solvent in vacuo yielded a pale yellow residue, which was dissolved in toluene (40 mL) to give a cloudy, pale yellow solution. The supernatant was decanted from the white precipitate of LiCl to give a clear, golden yellow solution. Removal of solvent under vacuum followed by recrystallization by toluene/hexane layering at 0 °C (2 days) yielded colorless crystals of **5** (0.52 g, 0.71 mmol, 79%); mp 194–196 °C. Anal. Calcd for C<sub>34</sub>H<sub>52</sub>N<sub>4</sub>P<sub>3</sub>S<sub>2</sub>: C, 55.38; H, 7.11; N, 7.60. Found: C, 55.65; H, 7.26; N, 7.20. <sup>1</sup>H NMR (C<sub>6</sub>D<sub>6</sub>,  $\delta$ ): 7.59 (br m, 15H, PPh<sub>3</sub>), 3.09 (s, NH), 1.91 (s, 18H, <sup>t</sup>Bu), 1.44 (s, 9H, <sup>t</sup>Bu), 1.38 (s, 9H, <sup>t</sup>Bu). <sup>31</sup>P{<sup>1</sup>H} NMR (C<sub>6</sub>D<sub>6</sub>,  $\delta$ ): 36.0 [d, <sup>2</sup>J(<sup>31</sup>P–<sup>31</sup>P) = 19 Hz], 24.8 [d, <sup>2</sup>J(<sup>31</sup>P–<sup>31</sup>P) = 19 Hz], 5.7 (br s, PPh<sub>3</sub>). IR (cm<sup>-1</sup>): 3391 [ $\nu$  (N–H)]. MS [EI, *m/z* (rel int)]: 737 (89) (M<sup>+</sup>).

**Preparation of {Ni[(<sup>t</sup>BuN)(S)P( $\mu$ -N'<sup>t</sup>Bu)<sub>2</sub>P(S)(NH<sup>t</sup>Bu)]<sub>2</sub> (**6**).** A red solution of NiCl<sub>2</sub>(PEt<sub>3</sub>)<sub>2</sub> (0.16 g, 0.44 mmol) in THF (30 mL) was added to a stirred solution of {(THF)<sub>2</sub>Li[(<sup>t</sup>BuN)(S)P( $\mu$ -N'<sup>t</sup>Bu)<sub>2</sub>P(S)(NH<sup>t</sup>Bu)]} (0.50 g, 0.89 mmol) in THF (25 mL) at 23 °C to give a dark purple solution, which was stirred for 18 h at 23 °C. Removal of the solvent in vacuo yielded a dark purple residue, which was dissolved in toluene (40 mL) to give a cloudy, dark purple solution. The supernatant was separated from LiCl by decantation, and solvent was removed in vacuo. Recrystallization by toluene/hexane layering at 0 °C (2 days) yielded purple-green crystals of **6** (0.33 g, 0.37 mmol, 83%); mp 110 °C. Anal. Calcd for C<sub>32</sub>H<sub>74</sub>N<sub>8</sub>P<sub>4</sub>NiS<sub>4</sub>: C, 43.58; H, 8.46; N, 12.71. Found: C, 43.41; H, 8.35; N, 12.22. <sup>1</sup>H NMR (CDCl<sub>3</sub>,  $\delta$ ): 12.6 (s, NH), 0.12 (br s, 54H, <sup>t</sup>Bu), –0.05 (s, 18H, <sup>t</sup>Bu). <sup>31</sup>P{<sup>1</sup>H} NMR (CDCl<sub>3</sub>,  $\delta$ ): 115.5 (br s). IR (cm<sup>-1</sup>): 3389 [ $\nu$  (N–H)]. MS [*m/z* (rel int)]: 880(71) (M<sup>+</sup>).

UV–vis [CH<sub>2</sub>Cl<sub>2</sub>;  $\lambda_{\max}$  in nm ( $\epsilon$  in M<sup>-1</sup> cm<sup>-1</sup>): 238 (7.7 × 10<sup>3</sup>), 291 (7.9 × 10<sup>3</sup>), 568 (1.6 × 10<sup>3</sup>), 610 (1.2 × 10<sup>3</sup>).

**Preparation of {(PPh<sub>3</sub>)<sub>2</sub>Cu[(<sup>t</sup>BuN)(S)P( $\mu$ -N'<sup>t</sup>Bu)<sub>2</sub>P(S)(NH<sup>t</sup>Bu)]} (**7**).** A solution of PdCl<sub>2</sub>(PPh<sub>3</sub>)<sub>2</sub> (0.17 g, 0.25 mmol) in THF (20 mL) was added to a stirred solution of {(THF)<sub>2</sub>Li[(<sup>t</sup>BuN)(S)P( $\mu$ -N'<sup>t</sup>Bu)<sub>2</sub>P(S)(NH<sup>t</sup>Bu)]} (0.28 g, 0.49 mmol) in THF (25 mL) at 23 °C. After 18 h, removal of the solvent in vacuo yielded a dark orange residue, which was dissolved in toluene (40 mL) to give a cloudy, dark orange solution. After removal of LiCl by decantation, solvent was removed in vacuo and the orange residue was recrystallized from toluene/hexane layering at 0 °C (2 days) to give **7** as a pale yellow solid (0.16 g, 0.25 mmol, 82%); mp 211–212 °C. Anal. Calcd for C<sub>34</sub>H<sub>52</sub>N<sub>4</sub>P<sub>3</sub>PdS<sub>2</sub>: C, 50.06; H, 6.43; N, 6.87. Found: C, 50.34; H, 6.72; N, 6.69. <sup>1</sup>H NMR (C<sub>6</sub>D<sub>6</sub>,  $\delta$ ): 7.83 (br m, 15H, PPh<sub>3</sub>), 2.96 (s, NH), 1.82 (s, 9H, <sup>t</sup>Bu), 1.73 (s, 18H, <sup>t</sup>Bu), 1.28 (s, 9H, <sup>t</sup>Bu). <sup>31</sup>P{<sup>1</sup>H} NMR (*d*<sub>8</sub>-THF,  $\delta$ ): 33.5 [d, <sup>2</sup>J(<sup>31</sup>P–<sup>31</sup>P) = 22 Hz], 26.3 [d, PPh<sub>3</sub>, <sup>3</sup>J(<sup>31</sup>P–<sup>31</sup>P) = 38 Hz], 19.7 [d of d, <sup>2</sup>J(<sup>31</sup>P–<sup>31</sup>P) = 22 Hz, <sup>3</sup>J(<sup>31</sup>P–<sup>31</sup>P) = 38 Hz]. IR (cm<sup>-1</sup>): 3382 [ $\nu$  (N–H)].

**Preparation of {Pd[(<sup>t</sup>BuN)(S)P( $\mu$ -N'<sup>t</sup>Bu)<sub>2</sub>P(S)(NH<sup>t</sup>Bu)]<sub>2</sub> (**8**).** A solution of PdCl<sub>2</sub>(PhCN)<sub>2</sub> (0.17 g, 0.44 mmol) in THF (30 mL) was added to a stirred solution of {(THF)<sub>2</sub>Li[(<sup>t</sup>BuN)(S)P( $\mu$ -N'<sup>t</sup>Bu)<sub>2</sub>P(S)(NH<sup>t</sup>Bu)]} (0.50 g, 0.89 mmol) in THF (20 mL) at 23 °C. After 18 h, removal of the solvent in vacuo yielded a brown residue, which was dissolved in toluene (40 mL) to give a cloudy, brown solution. LiCl was removed by decantation, and solvent was removed in vacuo. Recrystallization of the residue by toluene/hexane layering at 0 °C (2 days) yielded pale yellow crystals of **8** (0.30 g, 0.32 mmol, 72%); mp 264–266 °C. Anal. Calcd for C<sub>30</sub>H<sub>82</sub>N<sub>8</sub>P<sub>4</sub>PdS<sub>4</sub>: C, 45.85; H, 8.09; N, 10.97. Found: C, 45.55; H, 8.02; N, 10.57. <sup>1</sup>H NMR (C<sub>6</sub>D<sub>6</sub>,  $\delta$ ): 2.85 (s, NH), 1.75 (s, 36H, <sup>t</sup>Bu), 1.44 (s, 18H, <sup>t</sup>Bu), 1.30 (s, 18H, <sup>t</sup>Bu). <sup>31</sup>P{<sup>1</sup>H} NMR (*d*<sub>8</sub>-THF,  $\delta$ ): 37.6 [d, <sup>2</sup>J(<sup>31</sup>P–<sup>31</sup>P) = 25 Hz], 26.9 [d, <sup>2</sup>J(<sup>31</sup>P–<sup>31</sup>P) = 25 Hz]. IR (cm<sup>-1</sup>): 3398 [ $\nu$  (N–H)], MS [EI, *m/z* (rel int)]: 929 (20) (M<sup>+</sup>).

**Preparation of {(PEt<sub>3</sub>)<sub>2</sub>Pt[(<sup>t</sup>BuN)(S)P( $\mu$ -N'<sup>t</sup>Bu)<sub>2</sub>P(S)(NH<sup>t</sup>Bu)]} (**9**).** A solution of *cis*-PtCl<sub>2</sub>(PEt<sub>3</sub>)<sub>2</sub> (0.22 g, 0.44 mmol) in THF (30 mL) was added to a stirred solution of {(THF)<sub>2</sub>Li[(<sup>t</sup>BuN)(S)P( $\mu$ -N'<sup>t</sup>Bu)<sub>2</sub>P(S)(NH<sup>t</sup>Bu)]} (0.50 g, 0.89 mmol) in THF (25 mL) at 23 °C. After 18 h, removal of the solvent in vacuo yielded a golden-yellow residue that was redissolved in toluene (40 mL) to give a cloudy, golden-yellow solution. After removal of LiCl and solvent, the residue was recrystallized from toluene/hexane by layering at 0 °C (2 days) to give pale yellow crystals of **9** (0.33 g, 0.39 mmol, 87%); mp 102–104 °C (dec). Anal. Calcd for C<sub>34</sub>H<sub>72</sub>N<sub>4</sub>P<sub>4</sub>PtS<sub>2</sub>: C, 44.38; H, 7.89; N, 6.09. Found: C, 42.15; H, 7.59; N, 6.24. <sup>1</sup>H NMR (*d*<sub>8</sub>-THF,  $\delta$ ): 2.13 (q, 12H, P(CH<sub>2</sub>CH<sub>3</sub>)), 1.54 (s, 18H, <sup>t</sup>Bu), 1.31 (s, 18H, <sup>t</sup>Bu), 1.16 (t, 18H, P(CH<sub>2</sub>CH<sub>3</sub>)). <sup>31</sup>P{<sup>1</sup>H} NMR (*d*<sub>8</sub>-THF,  $\delta$ ): 8.5 [d, <sup>3</sup>J(<sup>31</sup>P–<sup>31</sup>P) = 28 Hz, <sup>1</sup>J(<sup>31</sup>P–<sup>195</sup>Pt) = 2857 Hz], –30.8 [d, <sup>3</sup>J(<sup>31</sup>P–<sup>31</sup>P) = 28 Hz, <sup>2</sup>J(<sup>31</sup>P–<sup>195</sup>Pt) = 98 Hz]. <sup>195</sup>Pt NMR (*d*<sub>8</sub>-THF,  $\delta$ ): –4699.2 [t of t, <sup>2</sup>J(<sup>195</sup>Pt–<sup>31</sup>P) = 117 Hz, <sup>1</sup>J(<sup>31</sup>P–<sup>195</sup>Pt) = 2846 Hz]. MS [*m/e* (rel int)]: 841 (44) (M<sup>+</sup>).

**X-ray Analyses.** All measurements of **5**, **8**·C<sub>7</sub>H<sub>8</sub>, and **9**·C<sub>6</sub>H<sub>6</sub> were made on a Rigaku AFC6S diffractometer. The measurements for **6**·C<sub>7</sub>H<sub>8</sub> were carried out on a Bruker AXS P4/RA/SMART 1000 CCD diffractometer. Crystallographic data are summarized in Table 1. For structures **5**, **8**·C<sub>7</sub>H<sub>8</sub>, and **9**·C<sub>6</sub>H<sub>6</sub> scattering factors were those of Cromer and Waber<sup>9</sup> and allowance was made for anomalous dispersion.<sup>10</sup> All calculations were performed using teXsan<sup>11</sup> and refinements carried out with the aid of SHELXL-97.<sup>12a</sup>

**5.** A colorless prismatic crystal of {(PPh<sub>3</sub>)<sub>2</sub>Cu[(<sup>t</sup>BuN)(S)P( $\mu$ -N'<sup>t</sup>Bu)<sub>2</sub>P(S)(NH<sup>t</sup>Bu)]} (0.50 mm × 0.48 mm × 0.30 mm) was mounted on a

(8) Jensen, K. A. Z. *Anorg. Allg. Chem.* **1936**, 229, 265.(9) Cromer, D. T.; Waber, J. T. *International Tables for Crystallography*; Kynoch Press: Birmingham, England, 1974; Vol. IV, Table 2.2A, pp 71–98.(10) Ibers, J. A.; Hamilton, W. C. *Acta Crystallogr.* **1964**, 17, 781.(11) teXsan: *Crystal Structure Analysis Package*; Molecular Structure Corp.: The Woodlands, TX, 1985, 1992.(12) (a) Sheldrick, G. M. *SHELX97, Program for the Solution of Crystal Structures*; University of Göttingen: Göttingen, Germany, 1997. (b) Sheldrick, G. M. *SHELX97-2, Program for the Solution of Crystal Structures*; University of Göttingen: Göttingen, Germany, 1997.

**Table 1.** Crystallographic Data for **5**, **6**·C<sub>7</sub>H<sub>8</sub>, **8**·C<sub>7</sub>H<sub>8</sub>, and **9**·C<sub>7</sub>H<sub>8</sub>

	<b>5</b>	<b>6</b> ·C <sub>7</sub> H <sub>8</sub>	<b>8</b> ·C <sub>7</sub> H <sub>8</sub>	<b>9</b> ·C <sub>7</sub> H <sub>8</sub>
formula	C <sub>34</sub> H <sub>52</sub> CuN <sub>4</sub> P <sub>3</sub> S <sub>2</sub>	C <sub>39</sub> H <sub>82</sub> N <sub>8</sub> NiP <sub>4</sub> S <sub>4</sub>	C <sub>39</sub> H <sub>82</sub> N <sub>8</sub> P <sub>4</sub> PdS <sub>4</sub>	C <sub>34</sub> H <sub>72</sub> N <sub>4</sub> P <sub>4</sub> PtS <sub>2</sub>
fw	737.37	973.96	1021.65	920.05
space group	<i>P</i> <sub>2</sub> / <i>c</i>	<i>Pbcn</i> (No. 60)	<i>P</i> <sub>2</sub> / <i>n</i>	<i>P</i> <sub>2</sub> / <i>n</i> (No. 14)
<i>a</i> , Å	19.175(4)	14.298(5)	13.975(3)	12.479(6)
<i>b</i> , Å	20.331(4)	15.333(5)	14.283(3)	21.782(7)
<i>c</i> , Å	10.017(6)	24.378(5)	15.255(4)	17.048(5)
β, deg	91.79(3)		116.565(18)	100.30(3)
<i>V</i> , Å <sup>3</sup>	3903(2)	5344(3)	2723.5(11)	4559(3)
<i>Z</i>	4	4	2	4
<i>T</i> , K	170(2)	193(2)	170(2)	170(2)
λ, Å	0.71069	0.71073	0.71069	0.71069
<i>d</i> <sub>calcd</sub> , g cm <sup>-3</sup>	1.255	1.210	1.246	1.340
μ, mm <sup>-1</sup>	0.82	0.673	0.65	3.33
<i>F</i> (000)	1560	2096	1084	1896
<i>R</i> <sup>a</sup>	0.074	0.0371	0.047	0.059
<i>R</i> <sub>w</sub> <sup>b</sup>	0.154	0.0933 <sup>c</sup>	0.119	0.136

<sup>a</sup>  $R = \sum ||F_o| - |F_c|| / \sum |F_o|$ . <sup>b</sup>  $R_w = [\sum w(|F_o| - |F_c|)^2 / \sum w F_o^2]^{1/2}$ . <sup>c</sup>  $R_w = \{[\sum w(F_o^2 - F_c^2)^2] / [\sum w(F_o^2)^2]\}^{1/2}$  (all data).

glass fiber. Cell constants and an orientation matrix for data collection were obtained from a least-squares refinement using the setting angles of 24 carefully centered reflections in the range 18.25° < 2θ < 21.57°. Scans of (1.47 + 0.34 tan θ)° were made at a speed of 4.0°/min (in ω) to a maximum 2θ value of 50.0°. The intensities of 6844 unique reflections were measured, of which 4157 had *I* > 2.00σ(*I*). The non-hydrogen atoms were refined anisotropically; hydrogen atoms were included at geometrically idealized positions. The phenyl rings were included as regular hexagons using constrained C–C bond lengths of 1.39 Å.

**6**·C<sub>7</sub>H<sub>8</sub>. A purple-green platelike crystal of {Ni[(<sup>t</sup>BuN)(S)P(μ-N<sup>t</sup>Bu)<sub>2</sub>P(S)(NH<sup>t</sup>Bu)]<sub>2</sub>·C<sub>7</sub>H<sub>8</sub>} (0.60 mm × 0.40 mm × 0.14 mm) was mounted on a glass fiber. A total of 11808 reflections were collected, of which 3178 had *I* > 2.00σ(*I*). The structure was solved by direct methods<sup>13</sup> and refined by full-matrix least-squares methods on *F*<sup>2</sup> with SHELX97-2.<sup>12b</sup> The methyl group of the toluene molecule was disordered around the 2-fold axis; the atom C(1S) was refined with a partial occupancy factor of 0.50. The non-hydrogen atoms were refined anisotropically; hydrogen atoms were included at geometrically idealized positions but not refined. One of the hydrogen atoms of the toluene solvate was ignored due to the disordered methyl group.

**8**·C<sub>7</sub>H<sub>8</sub>. A yellow plate crystal of {Pd[(<sup>t</sup>BuN)(S)P(μ-N<sup>t</sup>Bu)<sub>2</sub>P(S)(NH<sup>t</sup>Bu)]<sub>2</sub>·C<sub>7</sub>H<sub>8</sub>} (0.43 mm × 0.36 mm × 0.17 mm) was mounted on a glass fiber. Cell constants and an orientation matrix for data collection were obtained from a least-squares refinement using the setting angles of 25 carefully centered reflections in the range 18.39° < 2θ < 23.08°. Scans of (1.52 + 0.34 tan θ)° were made at a speed of 4.0°/min to a maximum 2θ value of 50.0°. The intensities of 4813 unique reflections were measured, of which 2909 had *I* > 2.00σ(*I*). The non-hydrogen atoms were refined anisotropically; hydrogen atoms were included but not refined. A disordered molecule of toluene was located close to the inversion center, and its phenyl ring was refined as a regular hexagon during the early stages of refinements with isotropic C atoms and H atoms at fixed positions; during the final stages of refinements, toluene was not refined.

**9**·C<sub>7</sub>H<sub>8</sub>. A colorless prismatic crystal of {(PEt<sub>3</sub>)<sub>2</sub>Pt[(<sup>t</sup>BuN)(S)P(μ-N<sup>t</sup>Bu)<sub>2</sub>P(S)(N<sup>t</sup>Bu)]·C<sub>6</sub>H<sub>6</sub>} (0.48 mm × 0.40 mm × 0.20 mm) was mounted on a glass fiber. Cell constants and an orientation matrix for data collection were obtained from a least-squares refinement using the setting angles of 15 carefully centered reflections in the range 14.71° < 2θ < 17.46°. Scans of (1.31 + 0.34 tan θ)° were made at a speed of 4.0°/min to a maximum 2θ value of 50.1°. The intensities of 8028 unique reflections were measured, of which 4838 had *I* > 2.00σ(*I*). The data were corrected for Lorentz and polarization effects, and an empirical absorption correction was applied. The structure was solved by direct methods<sup>13</sup> and expanded using Fourier techniques.<sup>14</sup> The non-

hydrogen atoms were refined anisotropically. Hydrogen atoms were included but not refined. A disordered molecule of toluene was located in the lattice; C atoms of the solvate were refined with isotropic temperature factors using constrained C–C bond lengths of 1.39 Å.

## Results and Discussion

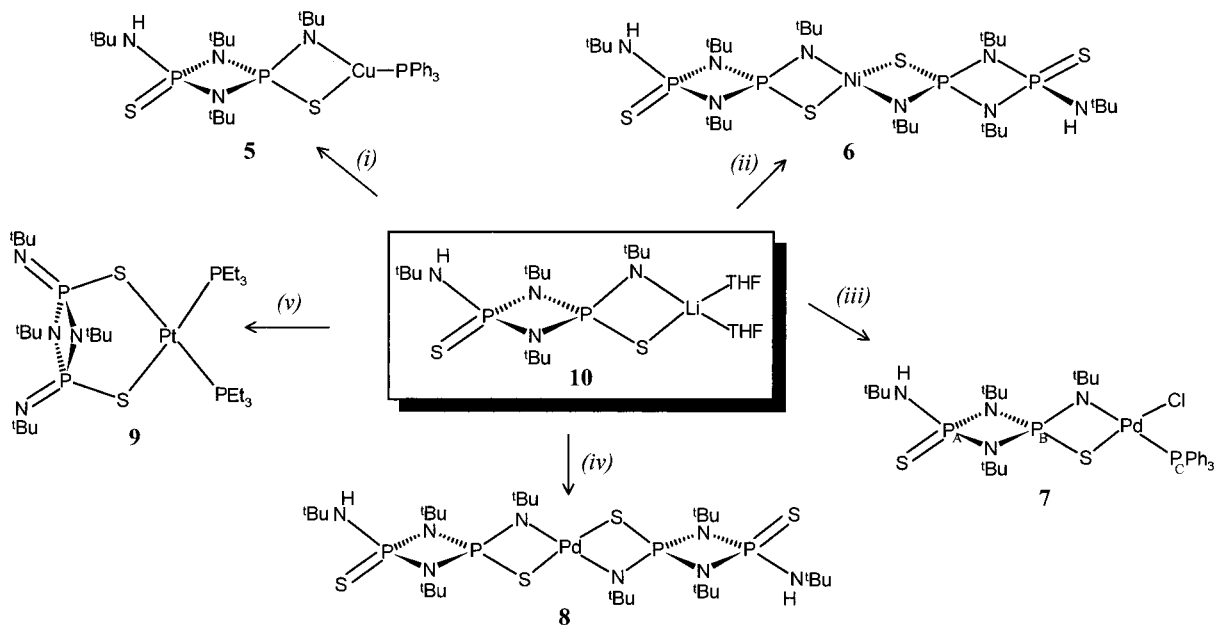
**Preparation and Spectroscopic Characterization of Cu(I), Ni(II), and Pd(II) Complexes of 1a and the Pt(II) Complex of 2a.** The monolithium derivative of **1a** (**10** in Scheme 2) is generated in essentially quantitative yield by the reaction of *cis*-[<sup>t</sup>Bu(H)N(S)P(μ-N<sup>t</sup>Bu)<sub>2</sub>P(S)N(H)<sup>t</sup>Bu]<sup>15</sup> with 1 equiv of Li<sup>n</sup>Bu in THF at 23 °C.<sup>6b</sup> The reaction of **10** with CuCl in acetonitrile, in the presence of triphenylphosphine, produced {(PPh<sub>3</sub>)Cu[(<sup>t</sup>BuN)(S)P(μ-N<sup>t</sup>Bu)<sub>2</sub>P(S)(NH<sup>t</sup>Bu)]} (**5**) in ca. 80% yield (Scheme 2). The <sup>31</sup>P NMR spectrum of **5** in C<sub>6</sub>D<sub>6</sub> reveals three distinct, and equally intense, phosphorus environments. Two mutually coupled doublets are observed at δ 36.0 and 24.8 [<sup>2</sup>*J*(<sup>31</sup>P–<sup>31</sup>P) = 19 Hz] (cf. δ (<sup>31</sup>P) = 36.5 and 16.9 [<sup>2</sup>*J*(<sup>31</sup>P–<sup>31</sup>P) = 21 Hz] for **10**);<sup>6b</sup> the third resonance is a broad singlet at δ 5.7. These data indicate the presence of a PPh<sub>3</sub> ligand and an *N,S* bonding mode for the anion **1a**. This conclusion is supported by the <sup>1</sup>H NMR spectrum of **5**, which exhibits three singlets at δ 1.91, 1.44, and 1.38, with relative intensities 2:1:1, attributed to the bridging N<sup>t</sup>Bu groups and the inequivalent terminal N<sup>t</sup>Bu groups, respectively. A broad multiplet centered at δ 7.59 (15H) is observed for the PPh<sub>3</sub> ligand, and a broad singlet at δ 3.09 is assigned to the NH proton. In the IR spectrum an NH stretching band is evident at 3391 cm<sup>-1</sup>, and the mass spectrum exhibited a strong molecular ion at *m/z* 737, consistent with the presence of one monoanion **1a** and one PPh<sub>3</sub> ligand.

The nickel(II) complex {Ni[(<sup>t</sup>BuN)(S)P(μ-N<sup>t</sup>Bu)<sub>2</sub>P(S)(NH<sup>t</sup>Bu)]<sub>2</sub>} (**6**) was obtained in 83% yield as purple-green crystals by the reaction of 2 equiv of **10** with NiCl<sub>2</sub>(PEt<sub>3</sub>)<sub>2</sub> in THF (Scheme 2). The <sup>31</sup>P NMR spectrum of **6** in CDCl<sub>3</sub> showed only a broad singlet at δ 115.5. We note that the related complex Ni[S(N<sup>t</sup>Pr)P(<sup>t</sup>Bu)<sub>2</sub>]<sub>2</sub>, which is tetrahedral in the solid state, shows an anomalous <sup>31</sup>P NMR chemical shift at δ 127 in C<sub>7</sub>H<sub>8</sub>.<sup>16</sup> The <sup>1</sup>H NMR spectrum of **6** consisted of two broad resonances at δ 0.12 and 0.05 with approximate relative inten-

(13) SIR97. Altomare, A.; Casciarano, G.; Giocovazzo, C.; Guagliardi, A.; Moliterni, A. G. G.; Burla, M. C.; Moliterni, G.; Camalli, M.; Spagna, R. *J. Appl. Crystallogr.* **1993**, *26*, 343.

(14) DIRDIF94. Beurskens, P. T.; Admiraal, G.; Beurskens, G.; Bosman, W. P.; de Gelder, R.; Israel, R.; Smits, J. M. M. The DIRDIF program system. Technical Report of the Crystallography Laboratory; University of Nijmegen: Nijmegen, The Netherlands, 1994.

(15) Hill, T. G.; Haltiwanger, R. C.; Thompson, M. L.; Katz, S. A.; Norman, A. D. *Inorg. Chem.* **1994**, *33*, 1770.

Scheme 2<sup>a</sup>

<sup>a</sup> (i) CuCl, PPh<sub>3</sub>, MeCN/PhMe, 23 °C, 18 h; (ii) 0.5NiCl<sub>2</sub>(PEt<sub>3</sub>)<sub>2</sub>, THF/PhMe, 23 °C, 18 h; (iii) 0.5PdCl<sub>2</sub>(PPh<sub>3</sub>)<sub>2</sub>, THF/PhMe, 23 °C, 18 h; (iv) 0.5PdCl<sub>2</sub>(PhCN)<sub>2</sub>, THF/PhMe, 23 °C, 18 h; (v) 0.5PtCl<sub>2</sub>(PEt<sub>3</sub>)<sub>2</sub>, THF/PhMe, 23 °C, 18 h.

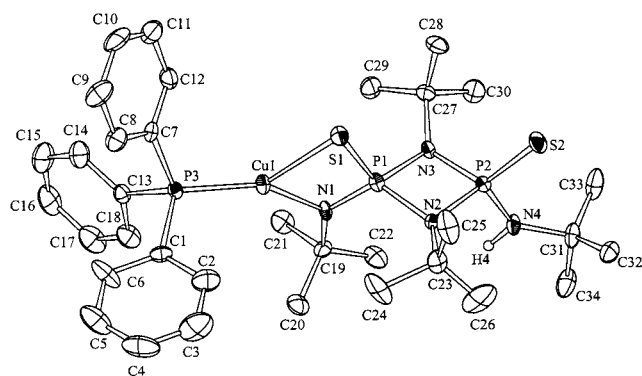


**Figure 1.** Molecular structure of  $\{(PPh_3)Cu[(^tBuN)(S)P(\mu-N^tBu)_2P(S)(NH^tBu)]\}$  (**5**). For clarity, the protons are omitted. Displacement ellipsoids are plotted at the 30% probability level.

sities 3:1. The broadness of the NMR resonances and the shift of the signals for *N*<sup>t</sup>Bu from the usual range of  $\delta$  (1.3–2.0) are indicative of a paramagnetic Ni(II) complex. The magnetic moment of **6** at 298 K is 2.90 BM. The IR spectrum of **6** showed an NH stretching band at 3389 cm<sup>-1</sup>, and the mass spectrum exhibited a strong molecular ion at *m/z* 880 consistent with the presence of two monoanionic ligands **1a** in the complex.

In contrast to the reaction of **10** with NiCl<sub>2</sub>(PEt<sub>3</sub>)<sub>2</sub>, the corresponding reaction with PdCl<sub>2</sub>(PPh<sub>3</sub>)<sub>2</sub> resulted in the replacement of only one chloride ligand to give  $\{(PPh_3)(Cl)Pd[(^tBuN)(S)P(\mu-N^tBu)_2P(S)(NH^tBu)]\}$  (**7**) as a pale yellow solid in 82% yield (Scheme 2). The <sup>31</sup>P NMR spectrum of **7** in *d*<sub>8</sub>-THF showed three equally intense resonances: a doublet at  $\delta$  33.5 [<sup>2</sup>*J*(<sup>31</sup>P–<sup>31</sup>P) = 22 Hz] (P<sub>A</sub>), a doublet at  $\delta$  26.3 [<sup>3</sup>*J*(<sup>31</sup>P–<sup>31</sup>P) = 38 Hz] (P<sub>C</sub>), and a doublet of doublets at  $\delta$  19.8 [<sup>2</sup>*J*(<sup>31</sup>P–<sup>31</sup>P) = 22 Hz, <sup>3</sup>*J*(<sup>31</sup>P–<sup>31</sup>P) = 38 Hz] (P<sub>B</sub>) (see Scheme 2 for assignments). Consistently the <sup>1</sup>H NMR spectrum of **7** in C<sub>6</sub>D<sub>6</sub> showed three resonances at  $\delta$  1.82, 1.73, and 1.28 in the

ratio 1:2:1 attributed to terminal, bridging, and terminal *N*<sup>t</sup>Bu groups, respectively. In addition, a multiplet is observed at  $\delta$  7.83 with an intensity corresponding to one PPh<sub>3</sub> ligand. A broad singlet attributed to the NH proton is apparent at  $\delta$  2.96, and the NH stretch in the IR spectrum is at 3382 cm<sup>-1</sup>.

By use of the more labile palladium(II) complex PdCl<sub>2</sub>(PhCN)<sub>2</sub> in the reaction with 2 equiv of **10** the compound  $\{Pd[(^tBuN)(S)P(\mu-N^tBu)_2P(S)(NH^tBu)]_2\}$  (**8**) was obtained as pale yellow crystals in 72% yield (Scheme 2). The <sup>31</sup>P NMR spectrum of **8** in *d*<sub>8</sub>-THF consists of two mutually coupled doublets centered at  $\delta$  37.6 and 26.9 [<sup>2</sup>*J*(<sup>31</sup>P–<sup>31</sup>P) = 25 Hz]. The <sup>1</sup>H NMR spectrum of **8** shows three resonances in the *N*<sup>t</sup>Bu region with relative intensities 2:1:1 together with a broad singlet at  $\delta$  2.85 for the NH protons. The NH stretch is observed at 3398 cm<sup>-1</sup> in the IR spectrum. Taken together the spectroscopic data indicate that **8** is a Pd(II) complex in which two ligands (**1a**) are *N,S*-coordinated to the metal.

In distinct contrast to the Ni(II) and Pd(II) chemistry, the treatment of *cis*-PtCl<sub>2</sub>(PEt<sub>3</sub>)<sub>2</sub> with 2 equiv of **10** produced the complex  $\{(PEt_3)_2Pt[(^tBuN)(S)P(\mu-N^tBu)_2P(S)(NH^tBu)]\}$  (**9**) as pale yellow crystals in 87% yield. Multinuclear (<sup>31</sup>P, <sup>195</sup>Pt, and <sup>1</sup>H) NMR spectra indicate that **9** contains the dianionic ligand **2a** bonded to Pt through the two sulfur atoms (Scheme 2). The <sup>31</sup>P NMR spectrum of **9** in *d*<sub>8</sub>-THF exhibits two equally intense doublets, both of which show <sup>195</sup>Pt satellites:  $\delta$  8.5 [<sup>3</sup>*J*(<sup>31</sup>P–<sup>31</sup>P) = 28 Hz, <sup>1</sup>*J*(<sup>31</sup>P–<sup>195</sup>Pt) = 2857 Hz] and  $\delta$  -30.8 [<sup>3</sup>*J*(<sup>31</sup>P–<sup>31</sup>P) = 28 Hz, <sup>2</sup>*J*(<sup>31</sup>P–<sup>195</sup>Pt) = 98 Hz] [cf. [Pt(PEt<sub>3</sub>)<sub>2</sub>{Ph<sub>2</sub>P(S)NP(S)Ph<sub>2</sub>}][PF<sub>6</sub>],  $\delta$  12.6 [<sup>1</sup>*J*(<sup>31</sup>P–<sup>195</sup>Pt) = 3099 Hz] and 36.1 [<sup>2</sup>*J*(<sup>31</sup>P–<sup>195</sup>Pt) = 60.5 Hz]].<sup>17</sup> The <sup>195</sup>Pt NMR spectrum of **9** in *d*<sub>8</sub>-THF exhibits the expected triplet of triplets centered at  $\delta$  -4699 [<sup>1</sup>*J*(<sup>31</sup>P–<sup>195</sup>Pt) = 2846 Hz, <sup>2</sup>*J*(<sup>31</sup>P–<sup>195</sup>Pt) = 117 Hz]. The <sup>1</sup>H NMR spectrum consists of two equally intense resonances at  $\delta$  1.54 and 1.31 corresponding to the two pairs of equivalent bridging and terminal *N*<sup>t</sup>Bu groups, respectively, in addition to resonances for the two PEt<sub>3</sub> ligands with the appropriate relative intensities. There was no indication of the

(16) (a) Frommel, T.; Peters, W.; Wunderlich, H.; Kuchen, W. *Angew. Chem., Int. Ed. Engl.* **1992**, *31*, 612. (b) Deeg, A.; Kuchen, W.; Langsch, D.; Mootz, D. Peters, W.; Wunderlich, H. *Z. Anorg. Allg. Chem.* **1991**, *606*, 119.

(17) Phillips, J. R.; Slawin, A. M. Z.; White, A. J. P.; Williams, D. J.; Woollins, J. D. *J. Chem. Soc., Dalton Trans.* **1995**, 2467.



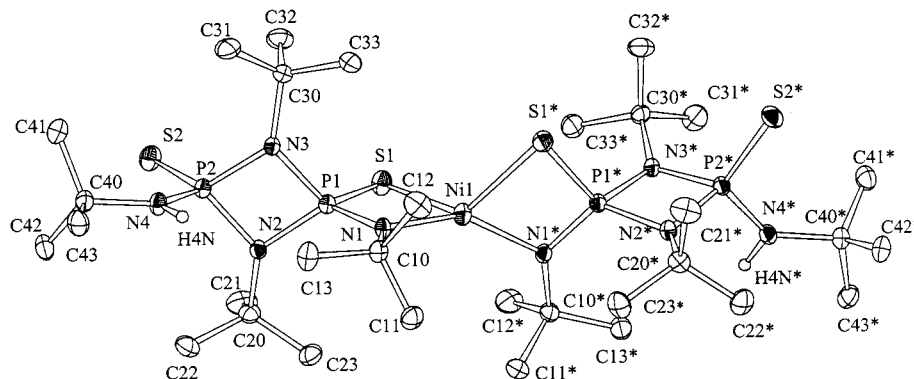


**Figure 2.** Molecular structure of  $\{\text{Ni}[(\text{tBuN})(\text{S})\text{P}(\mu\text{-N}^t\text{Bu})_2\text{P}(\text{S})(\text{NH}^t\text{Bu})]_2\}$  (**6**). For clarity, the protons are omitted. Displacement ellipsoids are plotted at the 30% probability level.

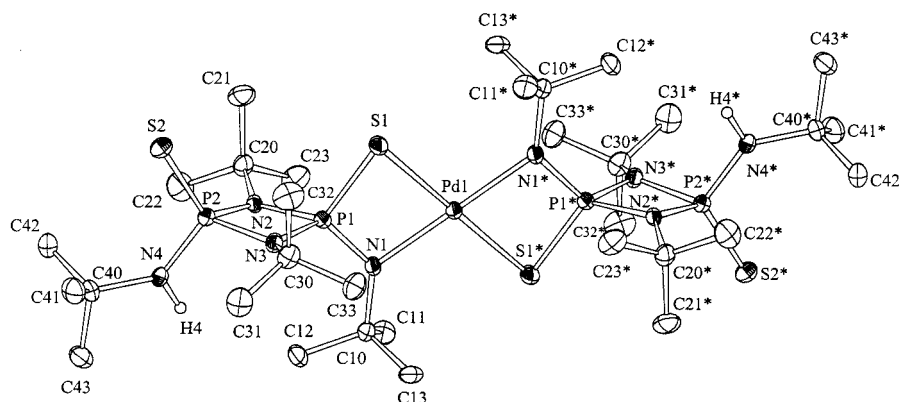


**Figure 3.** Molecular structure of  $\{\text{Pd}[(\text{tBuN})(\text{S})\text{P}(\mu\text{-N}^t\text{Bu})_2\text{P}(\text{S})(\text{NH}^t\text{Bu})]_2\}$  (**8**). For clarity, the protons are omitted. Displacement ellipsoids are plotted at the 30% probability level.

presence of NH groups in **9** from either the  $^1\text{H}$  NMR or IR spectra.

Thus the reaction of 2 equiv of **10** with  $\text{PtCl}_2(\text{PEt}_3)_2$  results in the formation of  $\text{LiCl}$  and elimination of  $\text{HCl}$  to generate the dianion **2a**, which coordinates in an  $S,S'$  fashion to Pt. The  $\text{HCl}$  eliminated apparently reacts with the second equivalent of **10** to produce *cis*- $[(\text{tBu}(\text{H})\text{N})(\text{S})\text{P}(\mu\text{-N}^t\text{Bu})_2\text{P}(\text{S})\text{N}(\text{H})^t\text{Bu})]$ , which was identified by  $^{31}\text{P}$  NMR. The complex **9** may also be prepared in essentially quantitative yield ( $^{31}\text{P}$  NMR) by the reaction of  $\text{PtCl}_2(\text{PEt}_3)_2$  with the dipotassium salt of **2a**.

**X-ray Structures of  $\{(\text{PPh}_3)\text{Cu}[(\text{tBuN})(\text{S})\text{P}(\mu\text{-N}^t\text{Bu})_2\text{P}(\text{S})(\text{NH}^t\text{Bu})]\}$  (**5**) and  $\{\text{M}[(\text{tBuN})(\text{S})\text{P}(\mu\text{-N}^t\text{Bu})_2\text{P}(\text{S})(\text{NH}^t\text{Bu})]_2\}$  (**6**,  $\text{M} = \text{Ni}$ ; **8**,  $\text{M} = \text{Pd}$ ).** The structures of **5**, **6**, and **8** were established by X-ray crystallography. The molecular geometry and atomic numbering scheme are shown in Figures 1–3, and pertinent structural parameters are summarized in Table 2. All three of these complexes display ( $N,S$ ) coordination of the monoanion **1a** to the metal. They differ, however, in their geometry at the metal center. In **5**, the three-coordinate copper(I) center has a distorted trigonal planar coordination sphere with an ( $N,S$ )-coordinated monoanion **1a** and one  $\text{PPh}_3$  ligand ( $\Sigma < \text{Cu} = 359.5^\circ$ ) (Figure 1). The nickel(II) complex **6** displays a distorted tetrahedral environment with  $N,S$ -coordination to two monoanions (Figure 2), whereas the palladium(II) derivative has a square planar arrangement of the two  $N,S$ -bonded ligands (Figure 3).

To the best of our knowledge, **5** represents the first example of a  $\text{CuNPS}$  heterocycle. The  $\text{Cu}-\text{N}$  distance is  $1.961(7)$  Å, a little shorter than the range of values for related ( $N,S$ )-bonded  $\text{Cu}$  complexes [ $1.991(5)$ – $2.052(5)$  Å];<sup>18</sup> whereas the  $\text{Cu}-\text{S}$  distance of  $2.391(3)$  Å is a little longer [ $2.263(2)$ – $2.299(2)$  Å].<sup>18</sup> The terminal  $\text{P}=\text{S}$  bond length of  $1.939(3)$  Å is almost identical

to the value of  $1.931(2)$  Å for  $(\text{TMEDA})\text{Li}[(\text{tBuN})(\text{S})\text{P}(\mu\text{-N}^t\text{Bu})_2\text{PN}(\text{H})^t\text{Bu}]$  (**11**)<sup>6b</sup> whereas the  $\text{P}-\text{S}$  bond in the  $\text{CuNPS}$  ring is lengthened to  $2.005(3)$  Å, significantly longer than the analogous bond in the  $\text{LiNPS}$  ring [ $1.978(2)$  Å].<sup>6b</sup> There is a similar disparity in the exocyclic  $\text{P}-\text{N}$  bond lengths [ $1.659(8)$  and  $1.584(7)$  Å, respectively; cf.  $1.641(5)$  and  $1.571(5)$  Å for the analogous bonds in **11**].<sup>6b</sup> Within the  $\text{P}_2\text{N}_2$  ring  $|d(\text{PN})| = 1.706(7)$  Å for the metalated side of the molecule and  $1.690(7)$  Å for the nonmetalated side [cf.  $1.713(5)$  and  $1.685(3)$  Å for **11**]. The bite angles ( $\angle\text{NPS}$ ) are  $103.7(3)^\circ$  and  $112.5(3)^\circ$  for the metalated and nonmetalated sides, respectively [cf.  $107.48(19)^\circ$  and  $112.0(2)^\circ$  in **11**].

The  $\text{Ni}(\text{II})$  and  $\text{Pd}(\text{II})$  complexes **6** and **8** both display  $N,S$ -coordination (Figures 2 and 3). Both  $\text{Ni}(\text{II})$  and  $\text{Pd}(\text{II})$  have a  $d^8$  configuration, but the nickel center in **6** attains a paramagnetic distorted tetrahedral environment whereas the palladium atom in **8** is in a diamagnetic square planar arrangement. Presumably a combination of the electronic properties of the monoanion **1a**, the bulky  $^t\text{Bu}$  groups, and the relatively small ionic radius of nickel favor the formation of a tetrahedral arrangement, even though, for four-coordinate  $\text{Ni}(\text{II})$  complexes, those with square planar geometries are the most common.<sup>19</sup>

There are several known thiophosphinate compounds which contain a  $\text{NiNPS}$  heterocycle whereas the  $\text{PdNPS}$  ring system is less common. The nickel complex **6** has a  $\text{Ni}-\text{N}$  distance of  $1.971(2)$  Å and a  $\text{Ni}-\text{S}$  distance of  $2.3449(9)$  Å [cf.  $1.947(1)$  and  $2.392(1)$  Å for  $[\text{R}_2\text{P}(\text{S})(\text{NR}')_2]\text{Ni}$  ( $\text{R} = ^t\text{Bu}$ ,  $\text{R}' = \text{cyclo}$

(18) (a) Abraham, S. P.; Narasimhamurthy, N.; Nethaji, M.; Samuelson, A. G. *Inorg. Chem.* **1993**, *32*, 1739. (b) Chan, C.-K.; Cheung, K.-K.; Che, C.-M. *Chem. Commun.* **1996**, 227.

(19) Greenwood, N.; Earnshaw, A. *Chemistry of the Elements*, 2nd ed.; Pergamon Press: New York, 1997; p 1157.

**Table 2.** Selected Bond Lengths (Å) and Bond Angles (deg) for { $(\text{PPh}_3)_3\text{Cu}[(^t\text{BuN})(\text{S})\text{P}(\mu\text{-N}^t\text{Bu})_2\text{P}(\text{S})(\text{NH}^t\text{Bu})]$ } (**5**), { $\text{Ni}[(^t\text{BuN})(\text{S})\text{P}(\mu\text{-N}^t\text{Bu})_2\text{P}(\text{S})(\text{NH}^t\text{Bu})]_2$ } (**6**), and { $\text{Pd}[(^t\text{BuN})(\text{S})\text{P}(\mu\text{-N}^t\text{Bu})_2\text{P}(\text{S})(\text{NH}^t\text{Bu})]_2$ } (**8**)

	<b>5</b> <sup>a</sup>	<b>6</b> ·C <sub>7</sub> H <sub>8</sub> <sup>b</sup>	<b>8</b> ·C <sub>7</sub> H <sub>8</sub> <sup>c</sup>
M(1)–N(1)	1.961(7)	1.971(2)	2.089(4)
M(1)–N(1)*		1.971(2)	2.089(4)
M(1)–S(1)	2.391(3)	2.3449(9)	2.3388(16)
M(1)–S(1)*		2.3449(9)	2.3388(16)
S(1)–P(1)	2.005(3)	2.0028(11)	2.006(2)
S(2)–P(2)	1.939(3)	1.9318(10)	1.933(2)
P(1)–N(1)	1.584(7)	1.592(2)	1.588(5)
P(1)–N(2)	1.707(7)	1.685(2)	1.697(4)
P(1)–N(3)	1.704(7)	1.687(2)	1.689(5)
P(2)–N(4)	1.659(8)	1.636(2)	1.637(5)
P(2)–N(2)	1.685(7)	1.698(2)	1.699(5)
P(2)–N(3)	1.694(7)	1.703(2)	1.699(5)
M(1)–P(3)	2.155(3)		
N(1)–M(1)–N(1)*		145.98(11)	180.000(1)
N(1)–M(1)–S(1)*		116.39(6)	102.48(13)
N(1)*–M(1)–S(1)*		80.55(6)	77.52(13)
N(1)–M(1)–S(1)	80.6(2)	80.55(6)	77.52(13)
N(1)*–M(1)–S(1)		116.39(6)	102.48(13)
S(1)*–M(1)–S(1)		122.76(4)	180.0
P(1)–S(1)–M(1)	75.86(10)	77.57(3)	81.37(7)
N(1)–P(1)–N(2)	120.1(4)	119.53(10)	120.5(3)
N(1)–P(1)–N(3)	119.5(4)	120.02(11)	121.4(3)
N(2)–P(1)–N(3)	82.3(3)	83.61(11)	83.6(2)
N(1)–P(1)–S(1)	103.7(3)	101.96(10)	100.67(18)
N(2)–P(1)–S(1)	115.2(3)	116.91(8)	115.64(18)
N(3)–P(1)–S(1)	115.9(3)	115.43(8)	115.89(19)
N(4)–P(2)–N(2)	107.4(4)	109.28(11)	108.5(2)
N(4)–P(2)–N(3)	110.2(4)	108.72(11)	109.3(2)
N(2)–P(2)–N(3)	83.3(3)	82.73(11)	83.2(2)
N(4)–P(2)–S(2)	112.5(3)	113.18(9)	113.35(19)
N(2)–P(2)–S(2)	120.9(3)	119.20(8)	119.68(18)
N(3)–P(2)–S(2)	119.1(3)	119.95(7)	119.07(19)
P(1)–N(1)–M(1)	99.6(4)	99.83(11)	100.4(2)
P(1)–N(2)–P(2)	96.9(4)	96.36(10)	95.9(2)
P(1)–N(3)–P(2)	96.7(4)	96.12(10)	96.2(2)
N(1)–M(1)–P(3)	149.2(2)		
S(1)–M(1)–P(3)	129.65(10)		

<sup>a</sup> M = Cu. <sup>b</sup> M = Ni. <sup>c</sup> M = Pd.

hexyl), **12**).<sup>16b</sup> The palladium complex **8** has Pd–N and Pd–S distances of 2.089(4) and 2.3388(16) Å, respectively [cf. 2.055(3) and 2.342(1) Å for  $[\text{R}_2\text{P}(\text{NR}')(\text{S})]_2\text{Pd}$  (R = OPh, R' = P(O)(OPh)<sub>2</sub>), **13**].<sup>20</sup> The terminal P=S and coordinated P–S bond lengths are very similar to those of **5** [cf. 1.9138(10) and 2.0028(11) Å in **6** and 1.933(2) and 2.006(2) Å in **8**, respectively].

The bite angles ( $\angle\text{NPS}$ ) are 77.57(3)° and 81.37(7)° for the metalated sides of **6** and **8**, respectively [cf. 102.1(1)° in **12** and 78.53(8)° in **13**]. Presumably, the wider bite angle in **8** is a result of the larger ionic radius of palladium. The large bite angle in **12** appears to be anomalous and may result from the lower steric demands of cyclohexyl groups attached to nitrogen atoms. The dissimilarity of the orientations of the two ligands around the metal centers in **6** and **8** is the only significant difference between the two complexes. Consideration of the bond angles at the metal centers (Table 2) indicates that **6** can be viewed as a highly distorted tetrahedral complex whereas **8** is a square planar complex in which the  $\angle\text{NPdS}$  bond angles are distorted by the constraints of the chelating ligand.

**X-ray Structure of  $\{(\text{PEt}_3)_2\text{Pt}[(^t\text{BuN})(\text{S})\text{P}(\mu\text{-N}^t\text{Bu})_2\text{P}(\text{S})(\text{N}^t\text{Bu})]\}$  (**9**).** The structure of **9** was established by X-ray crystallography. The molecular geometry and atomic numbering scheme are shown in Figure 4, and pertinent structural parameters are summarized in Table 3. The X-ray structure con-

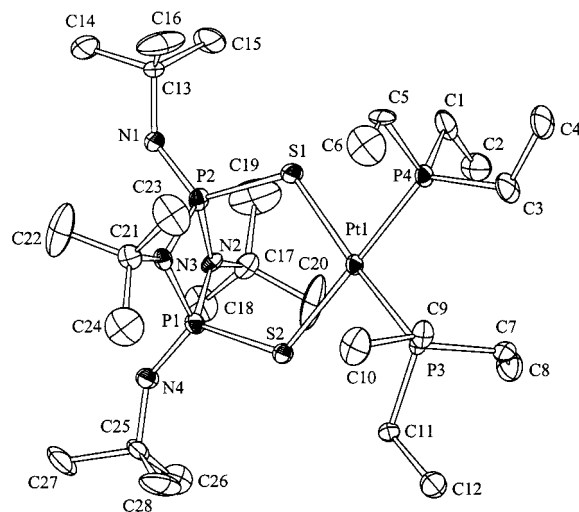


**Figure 4.** Molecular structure of  $\{(\text{PEt}_3)_2\text{Pt}[(^t\text{BuN})(\text{S})\text{P}(\mu\text{-N}^t\text{Bu})_2\text{P}(\text{S})(\text{N}^t\text{Bu})]\}$  (**9**). For clarity, the protons are omitted. Displacement ellipsoids are plotted at the 30% probability level.

**Table 3.** Selected Bond Lengths (Å) and Bond Angles (deg) for  $\{(\text{PEt}_3)_2\text{Pt}[(^t\text{BuN})(\text{S})\text{P}(\mu\text{-N}^t\text{Bu})_2\text{P}(\text{S})(\text{N}^t\text{Bu})]\}$  (**9**)

Pt(1)–P(3)	2.280(4)	P(2)–N(1)	1.518(12)
Pt(1)–P(4)	2.310(4)	P(2)–N(2)	1.681(11)
Pt(1)–S(1)	2.370(4)	P(2)–N(3)	1.683(12)
Pt(1)–S(2)	2.372(4)	P(1)–N(4)	1.523(13)
S(1)–P(2)	2.061(5)	P(1)–N(2)	1.674(12)
S(2)–P(1)	2.068(5)	P(1)–N(3)	1.713(13)
P(3)–Pt(1)–P(4)	96.53(14)	N(1)–P(2)–S(1)	115.8(5)
P(3)–Pt(1)–S(1)	174.27(16)	N(2)–P(2)–S(1)	107.0(5)
P(4)–Pt(1)–S(1)	78.79(14)	N(3)–P(2)–S(1)	109.9(4)
P(3)–Pt(1)–S(2)	85.24(14)	N(4)–P(1)–N(2)	116.1(7)
P(4)–Pt(1)–S(2)	177.01(15)	N(4)–P(1)–N(3)	119.1(7)
S(1)–Pt(1)–S(2)	99.57(13)	N(2)–P(1)–N(3)	83.1(6)
P(2)–S(1)–Pt(1)	114.2(2)	N(4)–P(1)–S(2)	116.8(5)
P(1)–S(2)–Pt(1)	114.1(2)	N(2)–P(1)–S(2)	109.9(4)
N(1)–P(2)–N(2)	118.9(7)	N(3)–P(1)–S(2)	106.9(4)
N(1)–P(2)–N(3)	117.0(6)	P(1)–N(2)–P(2)	95.7(6)
N(2)–P(2)–N(3)	83.8(6)	P(1)–N(3)–P(2)	94.1(6)

firms the conclusions based on the NMR data. Complex **9** is composed of the dianion **2a** bonded in an *S,S'* fashion to Pt with two  $\text{PEt}_3$  ligands in cis positions completing the distorted square planar geometry about Pt (bond angles are in the range 78.8–99.6°).

The mean Pt–S and Pt–P distances are 2.371(4) and 2.295(4) Å, respectively (cf. 2.341(4) and 2.408(4) Å in  $\text{Pt}(\text{PPh}_3)_2\text{-}(1,5\text{-Ph}_4\text{P}_2\text{N}_4\text{S}_2)$ ;<sup>21</sup> 2.393(3) in  $[\text{Pt}(\text{PEt}_3)_2\{\text{Ph}_2\text{P}(\text{S})\text{NP}(\text{S})\text{Ph}_2\}][\text{PF}_6]$ ).<sup>17</sup> The mean P–S distance is 2.065(5) Å, and the mean exocyclic P–N bond distance is 1.521(13) Å, indicative of double-bond character. The mean P–N bond length in the  $\text{P}_2\text{N}_2$  ring of 1.688(12) Å is similar to the corresponding distances in **5**, **6**, and **8** [range 1.681(11)–1.713(13)].

## Conclusions

Late transition metal derivatives of the monoanion  $[(^t\text{BuN})(\text{S})\text{P}(\mu\text{-N}^t\text{Bu})_2\text{P}(\text{S})(\text{NH}^t\text{Bu})]^-$  (**1a**) display *N,S*-coordination, whereas the dianion **2a** adopts an *S,S'* bonding mode toward platinum. The paramagnetic, tetrahedral Ni(II) complex **6** and the diamagnetic, square planar Pd(II) complex **8** represent good

(20) Zak, P. Z.; Fofana, M.; Kamenicek, J.; Glowiak, T. *Acta Crystallogr.* **1989**, *C45*, 1686.

(21) Chivers, T.; Edwards, M.; Meetsma, A.; van de Grampel, J. C.; van der Lee, A. *Inorg. Chem.* **1992**, *31*, 2156.

starting points for the synthesis of P<sub>2</sub>N<sub>2</sub>-templated coordination polymers with different metal centers via metalation reactions, e.g., with Me<sub>2</sub>M (M = Zn, Cd). Such experiments are in progress.

**Acknowledgment.** We thank the NSERC (Canada) for financial support, Dr. R. MacDonald (University of Alberta) for

assistance with the data collection for **6**·C<sub>7</sub>H<sub>8</sub>, and Prof. R. C. Thompson (U.B.C.) for the magnetic moment measurement.

**Supporting Information Available:** X-ray crystallographic files in CIF format for complexes **5**, **6**, **8**, and **9**. This material is available free of charge via the Internet at <http://pubs.acs.org>.

IC001173S